Anatomical and functional healing after resorbable magnesium scaffold implantation in human coronary vessels: A combined optical coherence tomography and quantitative flow ratio analysis

Catheterization & Cardiovascular Interventions

SCAI Society for Cardiovascular Angiography & Interventions

Anatomical and functional healing after Resorbable Magnesium Scaffold implantation in human coronary vessels: a combined optical coherence tomography and Quantitative Flow Ratio analysis.

Journal:	*Catheterization and Cardiovascular Interventions*
Manuscript ID	CCI-20-1361.R1
Wiley - Manuscript type:	Original Studies
Keywords:	OCT – Optical Coherence Tomography, QCA - Quantitative Coronary Angiography (QCA) , SBIO - Stent, Bioabsorbable, CAD - Coronary Artery Disease, PCI - Percutaneous Coronary Intervention (PCI)

Anatomical and functional healing after Resorbable Magnesium Scaffold implantation in human coronary vessels: a combined optical coherence tomography and Quantitative Flow Ratio analysis.

Enrico Cerrato[1], Davide Belliggiano[2], Giorgio Quadri[1], Andrea Erriquez[3], Matteo Anselmino[2], Alicia Quirós[4], Alfonso Franzè[1], Fabio Ferrari[1], Cristina Rolfo[1], Hernan Mejia-Renteria[5], Javier Escaned[5], Nieves Gonzalo[5], Gianluca Campo[3] and Ferdinando Varbella[1]

1.Interventional Cardiology Unit, San Luigi Gonzaga University Hospital, Orbassano and Rivoli Infermi Hospital, Rivoli (Turin), Italy

2.Division of Cardiology, "Città della Salute e della Scienza di Torino" Hospital, Department of Medical Sciences, University of Turin, Italy

3.Cardiovascular Institute, Azienda Ospedaliero-Universitaria di Ferrara, Cona, Italy; Maria Cecilia Hospital, GVM Care & Research, Cotignola (RA), Italy

4.Departmento de Matemáticas, Universidad de León, Spain

5.Cardiology Department, Hospital Clinico San Carlos, IDISSC & Universidad Complutense de Madrid, Madrid, Spain

Word count: 3381

Funding: none

Running title: QFR and OCT long term result after RMS Magmaris

Correspondence to: Dr. Enrico Cerrato, MD, Interventional Cardiology, San Luigi Gonzaga University Hospital, Orbassano and Infermi Hospital, Rivoli, Turin, Italy. E-mail: enrico.cerrato@gmail.com; www.cardiogroup.org.

ABSTRACT

Background. No data are currently available on the process of vessel healing and long-term physiological results after implantation of Resorbable Magnesium-made Scaffold (RMS) in human coronary arteries.

Objectives. To investigate after Percutaneous Coronary Intervention (PCI) and at 12 months follow-up (1) RMS resorption process and vessel healing, as judged by Optical Coherence Tomography (OCT) imaging; and (2) physiological result of RMS implantation evaluated by Quantitative Flow Ratio (QFR).

Methods. All patients successfully treated with at least one RMS from July 2016 to August 2018 at 2 Italian centers were evaluated. All cases with OCT pullback and/or coronary angiography suitable for QFR analysis performed after PCI and at 12 months were included. Resorption process was analysed at OCT in each frame reporting presence of residual struts in the vessel.

Results. Forty-four patients/forty-nine lesions were included. Twelve-months mean lumen area (LA; 7.54±3.04 mm^2) significantly decreased compared to mean LA recorded immediately after PCI (8.12±1.89 mm^2; $p < 0.01$). However, LA changes did not affect the functional result of PCI with a non-ischemic QFR value (>0.80) in 98% of cases at twelve-months follow-up. Protruding struts were detectable in more than half cases and their presence were correlated with an increase in mean LA (+0.73mm^2 [95% CI 0.51 - 0.94], $p<0.001$).

Conclusions. RMS implantation in a real-world population lead to significant decrease in mean LA without significant functional impairment. Two different patterns of RMS resorption were recorded, whose clinical significance remains to be investigated.

CONDENSED ABSTRACT

The aim of this study is to investigate the Resorbable Magnesium-made Scaffold (RMS) resorption process and vessel healing after PCI and at 12-months follow-up, as judged by Optical Coherence Tomography (OCT), and 12-months physiological result of RMS implantation, evaluated by Quantitative Flow Ratio (QFR). Forty-four patients with 49 lesions were analyzed. At 12-months, mean lumen area significantly decreased compared to post-PCI results (7.54±3.04mm^2 vs. 8.12±1.89mm^2; p<0.01); despite this, functional result of PCI was not impaired with a non-ischemic QFR value (>0.80) in 98% of cases at twelve-months follow-up. Moreover, two different patterns of RMS resorption were recorded, whose clinical significance remains to be investigated.

Abbreviations list

Optical Coherence Tomography (OCT)

Quantitative Flow Ratio (QFR)

Quantitative Coronary Angiography (QCA)

Fractional Flow Reserve (FFR)

Resorbable Magnesium Scaffold (RMS)

Percutaneous Coronary Intervention (PCI)

Lumen Area (LA)

Acute Coronary Syndrome (ACS)

Bioresorbable Scaffold (BRS)

INTRODUCTION

Bioresorbable scaffolds (BRS) can provide temporary mechanical support to coronary arteries without the long-term limitations of permanent metallic drug-eluting stents (DES).

The Resorbable Magnesium-based sirolimus-eluting Scaffold (RMS) Magmaris (Biotronik AG, Bülach, Switzerland) is the only metallic CE-marked resorbable scaffold currently available [1]. It was designed to provide a short-term lumen support (up to 3 months) before being completely bioresorbed by the vessel endothelium.[1]

Quantitative flow ratio (QFR), an angiography-derived FFR, has been validated as an accurate alternative to FFR in several studies and offers the advantage of allowing serial assessments based on angiography.[2–6]

Limited data are currently available on the process of vessel healing and on long-term physiological results after implantation of RMS in human coronary arteries[7–10]. An Optical Coherence Tomography (OCT) pattern of resorption characterized by a "bumpy" neointima due to the presence of multiple "humps" was described in a single case report [11] and the same pattern of protruding struts were recently described in 38% of cases at 1-year OCT evaluation in the MAGSTEMI-OCT study[12]. Incidence and implications of this pattern remain unexplored. Given these premises, the aim of this study is to investigate (i) RMS resorption process and vessel healing, as judged by Optical Coherence Tomography (OCT) imaging after PCI and at 12 months; and (ii) 12-months physiological result of RMS implantation evaluated by Quantitative Flow Ratio (QFR).

METHODS

Study population

All patients successfully treated with at least one RMS from July 2016 to August 2018 and included in the MAGnesIum Alloy Scaffold for Coronary Artery Disease trial (MAGIC: ClinicalTrials.gov identifier NCT04098042) were evaluated. The procedures were performed at two high-volume PCI centres in Italy (Degli Infermi Hospital, Rivoli, Turin and San Luigi Gonzaga University Hospital,

Orbassano, Turin) that share the same Interventional Cardiology team. The decision to implant RMS was at description of the operator and mainly based on patient's age and medical history. The RMS implantation was highly standardized and fulfilled the following indications: (i) mandatory pre-dilation, possibly until 1:1 ratio in respect to vessel diameter; (ii) OCT imaging highly suggested; (iii) RMS sizing based on intracoronary imaging; (iv) mandatory post-dilatation, possibly with non-compliant balloon. Dual antiplatelet therapy (DAT) with aspirin and $P2Y_{12}$ inhibitors was prescribed at discharged and recommended for at least 12 months. Follow-up protocol included clinical visits at 1 and 6 months and coronary angiography with OCT analysis at 12 months. The present analysis is focused on patients fulling the following criteria: (i) availability of OCT imaging and/or angiographic images suitable for QFR computation at the end of PCI and at 1-year follow-up procedure; (ii) uneventful 1-year follow-up; (iii). Records were excluded in case of any clinical events or one-year angiogram not performed or refused or when OCT were unavailable/incomplete or QFR analysis not feasible. All patients signed an informed consent for PCI with scaffold deployment and OCT guidance at the time of procedure. Data collection and analysis of acquired data was approved by the Independent Ethical Committee of San Luigi Gonzaga University Hospital.

Quantitative Coronary Angiography (QCA) and Quantitative Flow Ratio (QFR) analysis

Computation of Quantitative Coronary Angiography (QCA) and QFR were performed offline, using QAngio XA 3D (Medis Medical Imaging System, Leiden, the Netherlands) software. The following characteristics were estimated by QCA for each lesion: minimum lumen diameter (MLD), reference vessel diameter (RVD) and stenosis diameter. QFR computation was performed in agreement with the step-by-step procedure validated in previous studies [2–6,13]. In the present analysis, contrast QFR values were computed before PCI, immediately after PCI and at follow-up. The QFR value was calculated in the entire vessel, starting from the most proximal available segment until its diameter became less than 1.5 mm. QCA and QFR computation were performed in the core laboratory of the

University Hospital of Ferrara by two independent operators, certified for QCA and QFR computation.

Optical Coherence Tomography (OCT) acquisition and analysis

OCT images were acquired with commercially available systems (C7 System; LightLab Imaging Inc/St Jude Medical, Westford, MA; and after its availability, Optis System; Abbott Vascular). The OCT catheter was advanced to the distal end of the scaffold and the automatic pullback initiated concordantly with blood clearance. All OCT measurements were performed off-line using the proprietary software at the study site core laboratory by two experienced investigators (DB, MF) blinded to clinical data and not involved in PCI procedures and were externally supervised by a third investigator (NG) in the Hospital Clinico San Carlos, Madrid. OCT images were analyzed at 1 mm intervals and correspondent frames were analysed at one-year follow-up using the RMS tantallium markers as proximal and distal scaffold's references. Resorption process was analysed at OCT by counting any residual struts defined as bright structures with posterior shadow in each selected frame. Presence of protruding struts (intimal "humps") in the lumen were also registered. Complete resorption pattern with indiscernible struts was defined ad "golden tube" pattern.

Methodology used for QCA, QFR and OCT analysis, as well definition of each variable collected are summarized in **Supplemental material appendix.**

Statistical analysis

Continuous variables are summarized as mean ± standard deviation; categorical variables are provided as count (percentage%). The Kolmogorov–Smirnov test was performed to test for non-parametric normal distribution. Regarding the comparison of continuous variables, statistical differences between two groups were assessed either with a t-test or with a Mann–Whitney U-test, when appropriate. For categorical variables, a Chi-squared or Fisher's exact test was carried out. The coefficient of correlation of Pearson (r) was used to determine the strength of the linear relationship between two quantitative variables. Mixed effect regression models were used for frame-to-frame

analysis, in order to take into account the intra-subject variability as well as the inter-subject variability. Statistical analyses were performed using SPSS version 22.0 (IBM SPSS Statistics, IBM Corporation, Armonk, NY, USA), Graphpad prism 4 (La Jolla California USA) and R software (http://www.R-project.org). A two-sided $P < 0.050$ was considered significant.

RESULTS

Seventy-eight patients underwent implantation of at least one RMS under OCT guidance (**Figure A, suppl. material)**. Thirty-four (43%) of them were excluded from the analysis due to lack of good quality OCT imaging at index procedure (n=7), adequate projection for QFR computation at index procedure (n=9), refusal to repeat 1-year coronary artery angiography (n=14) or adverse event in the first year (n=4). Clinical and periprocedural characteristics of included/excluded patients and lesions were reported in **suppl. Material tables A and B**. Finally, the study population included 44 patients (including 49 lesions and a total number of 59 RMS) who underwent a scheduled coronary angiography at 1 year (mean follow-up 11.7±1.0 months; **Figure B, suppl. Material and Figure 1, Central illustration, panel A**).

Patient and procedural data

Main clinical and procedural features are summarized in **table 1 and 2**. The majority of patients were male (86.4%) with an average age of 55±7.5 years. Clinical risk factors showed a normal distribution with diabetics accounting for about one-fourth of cases. Nearly half of the cases were admitted to hospital with diagnosis of acute coronary syndromes with Left Anterior Descending being the most treated vessel (57%). Almost all lesions were type B2 or C (96%) with at least one overlapping BRS in 43% of cases and an average scaffold length of 34.9±17.8 mm. Predilatation and postdilatation were performed in 100% of cases using non-compliant balloon at high pressures in almost all cases. Intracoronary imaging was used to guide implantation in all cases.

Quantitative coronary angiography

Table 3 shows main QCA findings. Minimal Lumen Diameter (MLD) of 2.55±0.31mm recorded immediately after PCI decreased to a follow-up value of 2.33±0.29mm ($p<0.01$). Late Lumen Loss was 0.22±0.33mm.

Quantitative Flow Ratio

Mean QFR value at the end of index PCI was 0.97±0.06. The 93.6% of lesions showed good functional post-PCI outcome, defined as post-PCI value >0.89. At 1-year follow-up, despite significant changes in MLD as compared to index PCI, the functional result was not impaired (**Figure 1, Central illustration, panel C**). Mean QFR value was 0.95±0.05, with 98% of vessels presenting a QFR value above the cut-off of 0.80 and 89.4% of the vessels showing a QFR values >0.89 (p-value not significant for all comparisons with post index PCI).

Optical coherence tomography

Overall, OCT analysis accounted more than 2000 mm analysed. All data are collected in **Table 3.** At the end of PCI, OCT analysis showed a good immediate result of all implanted RMS (malapposition area = 0.03±0.23 mm^2), without scaffolds fractures or significant edge dissections. Mean lumen area (LA) and mean scaffold area (SA) after PCI were respectively 8.12 ± 1.89 and 8.08 ± 1.83 mm^2 ($p=0.6$). Overall, mean LA decreased significantly at follow-up (7.54±3.04 mm^2; $p<0.01$ for both comparisons), (**Table 3 and figure 2**). However, mean LA increase in 31% of cases (n= 415 frames) and volume gain in 9 of 42 lesions (21.4%).

Bioresorption process

OCT revealed the absence of persistent BRS struts at 12 months. A pattern characterized by indiscernible struts was found in 43.8% of frames. In the remaining ones, intimal protruding residual struts ("humps") were documented, although in the majority of frames less than five per mm (n=668;

86.9%) were observed (**table 3 and Figure 1, Central illustration, panel B**). The relationship between LA changes and resorption pattern was tested. When no residual struts were documented, mean LA loss was -1.08mm^2. Presence of residual struts in a frame was significantly correlated with a LA gain at follow-up (+0.73mm^2 [95% CI 0.51 - 0.94], p<0.001) and each additional "hump" was significantly correlated with an additional increase of +0.20mm^2 (95% CI 0.13 - 0.26; p<0.001). These findings were confirmed performing a per-scaffold analysis resulting in a significant relationship between Mean Lumen Gain and percentage of "humps" (Pearson's r = 0.45, p = 0.003) as between the overall volume gain and percentage of "humps" (Pearson's r = 0.41, p = 0.007; **figure 3**).

DISCUSSION

To the best of our knowledge this is the first work reporting a combined imaging OCT and QFR assessment and investigating anatomical and functional 12-months RMS healing in a real-world population. This is also the larger available sample with serial OCT analysis at one year.

The main findings of this study are the following: 1) despite the inclusion of more complex patient/lesions, the decrease in lumen area at 1 year was similar to those previously reported in a selected population; 2) the decrease in luminal area at follow-up did not lead to physiological impairment as showed by QFR analysis; 3) following RMS, human coronary arteries showed two different OCT patterns of vascular healing at 1 year. Residual protruding struts ("humps") were detectable in more than half of cases and their presence was correlated with an increase in mean lumen area.

Imaging data regarding the long-term result after RMS are currently very limited being mainly reported in the BIOSOLVE trials[7–10]. Angiographic performance reported at 12 months [7] showed a similar Late Lumen Loss (LLL) compared to our series (mean = 0.25 ± 0.22 mm^2 vs 0.22 ± 0.33 mm^2, respectively). A BIOSOLVE II sub-study [9] included OCT serial examination of 65

scaffolds at 6 months and 25 scaffolds at 12 months showing a significant decrease in Minimal Lumen Area (MLA) from 6.32 mm^2 at post-procedure to 4.53 mm^2 at 6 months with a small not significant increase to 4.81 mm^2 at 12 months. Substantial stability of LLL and MLA was reported at 36 months[14]. Given the very small number of patients included, as the authors stated, these findings should be interpreted with caution. In addition, complex patients/lesions were excluded according to the study protocol (i.e. Acute Coronary Syndrome (ACS) at presentation, three vessel disease, lesion length > 21 mm) and functional evaluation was not provided in that cohort.

Beyond data coming from BIOSOLVE studies, an OCT case series including 6 patients with follow-up was recently published by another group[15]. Compared to our study, all patients were stable and were treated with a single scaffold and 5 over 6 lesions were type B1 (ACC/AHA classification). Follow-up was obtained at one year in only one case while in the other cases it was inferior/equal to 8 months. Given these presumptions, mean lumen area decreased from 7.03 ± 1.91 to 6.82 ± 3.79 (absolute difference 0.22 ± 2.64) even being not significant due to the extremely low sample.

With the current work we widely extended available data to a longer follow-up. We provided data on vessel healing by a serial OCT analysis of 47 lesions with 59 scaffolds implanted in complex cases including very long lesions (mean 38.2 ± 17.2mm), multiple overlapping, single-scaffold bifurcations and more than half in the setting of ACS. Despite these differences our anatomical results are in line with previous reports of significant decrease in LA (MLA from 6.30mm^2 post PCI to 4.60mm^2 at 12 months).

Our work reports for the first time physiological insights after a successful vessel restoration therapy with magnesium scaffold. Saito et al[16] retrospectively performed a QFR analysis at 6-9 months (n=185) and up to 24 months (n=30) in patients treated with the Fantom bioresorbable scaffold. The study concluded that PCI with Fantom BRS improved functional ischemia at 6-9 months with a slight decrease in QFR values over 24 months (0.94±0.07 vs. 0.91±0.09 respectively, p=0.04).

Of note, in that study imaging results were not reported and QFR did not reflect the functional status after vessel healing, given that Fantom resorption process takes about 36 months.

Differently, in our study the combination of imaging and physiology allowed us to state that functional result of RMS implantations remained preserved in the long run. This is relevant because, accordingly, we exclude any residual ischemia occurring as a consequence of the significant reduction of LA over time. Interestingly, in both post-PCI and at follow-up QFR values were > 0.89 in 93.6% and 89.4% of cases, respectively (**table 3**). At this regard, a large prospective study from our group[17] recently documented that a post-PCI QFR ≤0.89 was associated with a 3-fold increase in risk for vessel-oriented composite endpoint (hazard ratio: 2.91; 95% CI: 1.63 - 5.19; $p < 0.001$).

With respect to resorption process, similarly with data reported in BIOSOLVE studies[9,14], at 12 months OCT was not able to detect any strut. Remarkably there were no cases of late acquired malapposition of visible intraluminal structures suggesting struts fractures (as a difference with reported data with Absorb)[18]. This occurred even when multiple scaffolds were implanted in overlapping or in the setting of ACS including STEMI patients. We detected presence of residual protruding struts in the lumen, recently named “humps”, in more than half of the cases. The clinical implications of this vessel healing pattern remain to be elucidated. It is possible that the two patterns reflect differences in timing of the resorption process that could be influenced by several factors including for example the subjacent plaque type.

Recently, the MAGSTEMI-OCT study[12] reported 1-year OCT follow-up data on 48 RMS implanted during Primary PCI (PPCI). MLA at 1-year was similar to our series (4.60±1.55 vs 3.92±2.02 mm^2) and indiscernible struts pattern was found in 33%. Interestingly, others patterns including integrate struts and protruding and malapposed struts were found in 23% and 6% of cases respectively while these two patterns were not detected in our serial examinations. This difference could be explained considering that stents implanted in the context of PPCI have been shown to exhibit larger malapposition while in our registry we included a larger number of RMS implanted in

all clinical scenarios with half of cases in stable settings and only 15% of cases presenting with STEMI. Importantly, in our series all RMS were implanted under OCT guidance while no OCT were performed in MAGSTEMI during implantation. This could support the importance of OCT-guided RMS implantation to avoid device undersizing or acute struts malapposition especially in complex PCI setting.

Impact on shear stress of protruding struts has been previously reported as a potential cause of scaffold failure with Absorb [19,20]but no data in this regard are available for RMS. Magnesium Scaffolds demonstrated an increased endothelialization process and decreased thrombogenicity at three and 28 days compared to Absorb preclinical studies data [21]; however there is no data about the risk of scaffold thrombosis due to residual humps and potential clinical implications for DAT duration. Current guidelines [22] consider prolonging DAT up to the presumed full absorption of the Bioresorbable Scaffold but this indication was substantially based on Poly-LLactic Acid scaffolds data[23,24]. Interestingly, in our study the presence of protruding struts was associated with less lumen area decrease at follow-up. It could be hypothesized that in this case struts had a slower resorption process and a delayed lack of radial force which implies a better maintenance of the lumen area obtained after scaffold implantation. Optimal timing of resorption to maintain an adequate radial force enough time to stabilize the lumen gain remains to be elucidated. Anyhow, technological improvement of next generations of RMS with increased radial force is advisable.

Limitations

This is a retrospective study including cases performed in two centers. Although all consecutive patients were screened, many lesions have not been included and this limitation has to be recognize. However, reviewing all cases included we have the privilege of analyze the largest cohort of serial OCT imaging performed after RMS implantation in a real world population contributing to expand the current knowledge about the resorption process given the scarce evidence regarding OCT findings at follow-up coming from trials. As detailed in methods, we conducted a rigorous screening reviewing all angiograms and OCT pullback finally including only patients with

high quality OCT pullback (entire RMS included in the pullback both at baseline and at follow-up, without artifacts) in order to provide precise and detailed data with a nearly perfect matching in frame-by-frame analysis after PCI and at 12-months. As a consequence, to respect the protocol, we had to exclude a part of our records. However, exploring clinical and periprocedural features of excluded / included records, no significant differences emerged (**Supp. Materials, tables A and B**). Secondly, QFR computation does not allow, to date, any consideration in terms of restoration of vessel motility or epicardial conductance. Moreover, QFR assessment after PCI of culprit vessel in ACS may be influenced by subtended microvascular dysfunction secondary to myocardium infarction[25]. Overall, our results should be considered as hypothesis generating and not conclusive but contribute to extend current data on magnesium-based resorbable sirolimus-eluting scaffold performance in complex settings [26–28].

Conclusion

The present study showed that RMS implantation in a real-world population is associated to significant decrease in the coronary lumen, without significant functional impairment at twelve months, as assessed by QFR. Two different OCT patterns of RMS resorption were recorded, whose clinical significance remains to be investigate.

Figures captions

Figure 1, **central illustration**. Panel A: study flow-chart. Panel B: Optical Coherence Tomography (OCT) imaging findings post PCI and at 1-year follow-up. Panel C: Quantitative Flow Ratio (QFR) findings post PCI and at 1-year follow-up. * chi-square p value is reported using 0.80 as QFR threshold for ischemia.

Figure 2: Imaging OCT findings. Left panel: boxplots for lumen / scaffold Area after PCI and at 1-year follow-up. Right panel: relative frequency distribution for lumen / scaffold area after PCI and at 1-year follow-up.

Figure 3. Left panel: distribution of the Lumen Area changing in mm^2 (Lumen Area at follow-up - Lumen Area post PCI) for each number of protruding residual struts observed in each OCT frame. Boxes indicate 25% and 75% percentiles and the inner line marks the median. A dotted black line indicates a null gain and the grey line with shadow depicts the smoothed conditional means of Lumen Area changing given the number of protruding struts and the corresponding confidence interval. Right panel: mean Lumen Area ($mm^{2)}$ changing versus percentage of protruding residual struts per scaffold. The grey line corresponds to the least squares regression line with confidence interval.

Figure A (Suppl material). **Optical Coherence Tomography (OCT) and Quantitative Flow Ratio (QFR) post-PCI analysis.** Picture A represents the angiographic result after Resorbable Magnesium Scaffold (RMS). The blue line shows the area of the vessel previously affected by stenosis where the scaffold was implanted. B: Post-PCI contrast QFR. C: Post-PCI OCT, longitudinal view. Picture C represents the longitudinal view of the area of the vessel where the scaffold was implanted, as seen using OCT. OCT images were analyzed at 1mm intervals, using tantallium BRS markers or struts as distal and proximal references of the scaffold. The vertical yellow lines show where the OCT trasversal images (D,E,F) are located along the vessel. D: Post-PCI OCT, trasversal view. Example of tantallium BRS marker, used as distal and proximal references of the scaffold to define the area of the vessel to analyze. E: Post-PCI OCT, trasversal view. OCT findings after the

implantation of a RMS. F: Post-PCI OCT, trasversal view. Lumen area, maximum diameter and minimum diameter were registered each millimeter.

Figure B (Suppl material). Optical Coherence Tomography (OCT) and Quantitative Flow Ratio (QFR) one-year follow-up analysis

Picture A represents the 1-year result after Resorbable Magnesium Scaffold (RMS) implantation. The blue line shows the area where the scaffold was implanted. B: Follow-up contrast QFR. C: Follow-up OCT, longitudinal view. Picture C represents the longitudinal view of the area of the vessel where the scaffold was implanted, as seen using OCT. OCT images were analyzed at 1mm intervals, using tantallium BRS markers or struts as distal and proximal references of the scaffold. The vertical yellow lines show where the OCT trasversal images (D,E,F) are located along the vessel. D: Follow-up OCT, trasversal view. Example of tantallium BRS marker, used as distal and proximal references of the scaffold to define the area of the vessel to analyze. E: Follow-up OCT, trasversal view. Lumen area, maximum diameter and minimum diameter were registered each millimeter. F: Follow-up OCT, trasversal view. Presence of residual or protruding struts or in the vessel lumen was registered.

Disclosures: GQ received speaker fees from Biotronik in educational meetings. JE received speaker fees from Philips in educational meetings. Other authors have no conflict of interest to declare

Acknowledgments: The authors wish to thank Mattia Fuda for his valuable contribution to imaging OCT data analysis.

REFERENCES

1. Cerrato E, Barbero U, Gil Romero JA, Quadri G, Mejia-Renteria H, Tomassini F, Ferrari F, Varbella F, Gonzalo N, Escaned J. Magmaris™ resorbable magnesium scaffold: state-of-art review. *Future Cardiol*. 2019;15:267–79.
2. Tu S, Westra J, Yang J, von Birgelen C, Ferrara A, Pellicano M, Nef H, Tebaldi M, Murasato Y, Lansky A, Barbato E, van der Heijden LC, Reiber JHC, Holm NR, Wijns W, FAVOR Pilot Trial Study Group. Diagnostic Accuracy of Fast Computational Approaches to Derive Fractional Flow Reserve From Diagnostic Coronary Angiography: The International Multicenter FAVOR Pilot Study. *JACC Cardiovasc Interv*. 2016;9:2024–35.
3. Westra J, Andersen BK, Campo G, Matsuo H, Koltowski L, Eftekhari A, Liu T, Di Serafino L, Di Girolamo D, Escaned J, Nef H, Naber C, Barbierato M, Tu S, Neghabat O, Madsen M, Tebaldi M, Tanigaki T, Kochman J, Somi S, Esposito G, Mercone G, Mejia-Renteria H, Ronco F, Bøtker HE, Wijns W, Christiansen EH, Holm NR. Diagnostic Performance of In-Procedure Angiography-Derived Quantitative Flow Reserve Compared to Pressure-Derived Fractional Flow Reserve: The FAVOR II Europe-Japan Study. *J Am Heart Assoc*. 2018;7.
4. Xu B, Tu S, Qiao S, Qu X, Chen Y, Yang J, Guo L, Sun Z, Li Z, Tian F, Fang W, Chen J, Li W, Guan C, Holm NR, Wijns W, Hu S. Diagnostic Accuracy of Angiography-Based Quantitative Flow Ratio Measurements for Online Assessment of Coronary Stenosis. *J Am Coll Cardiol*. 2017;70:3077–87.
5. Kogame N, Takahashi K, Tomaniak M, Chichareon P, Modolo R, Chang CC, Komiyama H, Katagiri Y, Asano T, Stables R, Fath-Ordoubadi F, Walsh S, Sabaté M, Davies JE, Piek JJ, van Geuns R-J, Reiber JHC, Banning AP, Escaned J, Farooq V, Serruys PW, Onuma Y. Clinical Implication of Quantitative Flow Ratio After Percutaneous Coronary Intervention for 3-Vessel Disease. *JACC Cardiovasc Interv*. 2019;12:2064–75.
6. Spitaleri G, Tebaldi M, Biscaglia S, Westra J, Brugaletta S, Erriquez A, Passarini G, Brieda A, Leone AM, Picchi A, Ielasi A, Girolamo DD, Trani C, Ferrari R, Reiber JHC, Valgimigli M, Sabatè M, Campo G. Quantitative Flow Ratio Identifies Nonculprit Coronary Lesions Requiring Revascularization in Patients With ST-Segment-Elevation Myocardial Infarction and Multivessel Disease. *Circ Cardiovasc Interv*. 2018;11:e006023.
7. Haude M, Ince H, Abizaid A, Toelg R, Lemos PA, von Birgelen C, Christiansen EH, Wijns W, Neumann F-J, Kaiser C, Eeckhout E, Lim ST, Escaned J, Onuma Y, Garcia-Garcia HM, Waksman R. Sustained safety and performance of the second-generation drug-eluting absorbable metal scaffold in patients with de novo coronary lesions: 12-month clinical results and angiographic findings of the BIOSOLVE-II first-in-man trial. *Eur Heart J*. 2016;37:2701–9.
8. Haude M, Ince H, Kische S, Abizaid A, Tölg R, Alves Lemos P, Van Mieghem NM, Verheye S, von Birgelen C, Christiansen EH, Wijns W, Garcia-Garcia HM, Waksman R. Sustained safety and clinical performance of a drug-eluting absorbable metal scaffold up to 24 months: pooled outcomes of BIOSOLVE-II and BIOSOLVE-III. *EuroIntervention J Eur Collab Work Group Interv Cardiol Eur Soc Cardiol*. 2017;13:432–9.
9. Garcia-Garcia HM, Haude M, Kuku K, Hideo-Kajita A, Ince H, Abizaid A, Tölg R, Lemos PA, von Birgelen C, Christiansen EH, Wijns W, Escaned J, Dijkstra J, Waksman R. In vivo serial invasive imaging of the second-generation drug-eluting absorbable metal scaffold (Magmaris — DREAMS 2G) in de novo coronary lesions: Insights from the BIOSOLVE-II First-In-Man Trial. *Int J Cardiol*. 2018;255:22–8.
10. Haude M, Ince H, Abizaid A, Toelg R, Lemos PA, von Birgelen C, Christiansen EH, Wijns W, Neumann F-J, Kaiser C, Eeckhout E, Lim ST, Escaned J, Garcia-Garcia HM, Waksman R. Safety and performance of the second-generation drug-eluting absorbable metal scaffold in patients with de-novo coronary artery lesions (BIOSOLVE-II): 6 month results of a prospective, multicentre, non-randomised, first-in-man trial. *Lancet Lond Engl*. 2016;387:31–9.

11. Alfonso F, Cuesta J, García-Guimaraes M, Rivero F. "Bumpy" neointima: the fingerprint of bioabsorbable magnesium scaffold resorption. *EuroIntervention*. 2019;15:e380–1.
12. Gomez-Lara J, Ortega-Paz L, Brugaletta S, Cuesta J, Romaní S, Serra A, Salinas P. Bioresorbable scaffolds versus permanent sirolimus- eluting stents in patients with ST-Segment Elevation Myocardial Infarction: vascular healing outcomes from the MAGSTEMI trial n.d.:28.
13. Mejía-Rentería H, Lauri FM, Lee JM, McInerney A, van der Hoeven NW, de Waard GA, Fernández-Ortiz A, Macaya C, Knaapen P, van Royen N, Koo B-K, Escaned J. Interindividual Variations in the Adenosine-Induced Hemodynamics During Fractional Flow Reserve Evaluation: Implications for the Use of Quantitative Flow Ratio in Assessing Intermediate Coronary Stenoses. *J Am Heart Assoc*. 2019;8:e012906.
14. Haude M, Ince H, Toelg R, Lemos PA, von Birgelen C, Christiansen EH, Wijns W, Neumann F-J, Eeckhout E, Garcia-Garcia HM, Waksman R. Safety and performance of the second-generation drug-eluting absorbable metal scaffold (DREAMS 2G) in patients with de novo coronary lesions: three-year clinical results and angiographic findings of the BIOSOLVE-II first-in-man trial. *EuroIntervention J Eur Collab Work Group Interv Cardiol Eur Soc Cardiol*. 2020;15:e1375–82.
15. Tovar Forero MN, Zandvoort L, Masdjedi K, Diletti R, Wilschut J, Jaegere PP, Zijlstra F, Van Mieghem NM, Daemen J. Serial invasive imaging follow-up of the first clinical experience with the Magmaris magnesium bioresorbable scaffold. *Catheter Cardiovasc Interv*. 2020;95:226–31.
16. Long-term serial functional evaluation after implantation of the Fantom sirolimus-eluting bioresorbable coronary scaffold - Saito - - Catheterization and Cardiovascular Interventions - Wiley Online Library n.d. https://onlinelibrary-wiley-com.bvsp.idm.oclc.org/doi/epdf/10.1002/ccd.28804 (accessed 1 March 2020).
17. Biscaglia S, Tebaldi M, Brugaletta S, Cerrato E, Erriquez A, Passarini G, Ielasi A, Spitaleri G, Girolamo DD, Mezzapelle G, Geraci S, Manfrini M, Pavasini R, Barbato E, Campo G. Prognostic Value of QFR Measured Immediately After Successful Stent Implantation: The International Multicenter Prospective HAWKEYE Study. *JACC Cardiovasc Interv*. 2019;12:2079–88.
18. Gori T, Jansen T, Weissner M, Foin N, Wenzel P, Schulz E, Cook S, Münzel T. Coronary evaginations and peri-scaffold aneurysms following implantation of bioresorbable scaffolds: incidence, outcome, and optical coherence tomography analysis of possible mechanisms. *Eur Heart J*. 2016;37:2040–9.
19. Thondapu V, Tenekecioglu E, Poon EKW, Collet C, Torii R, Bourantas CV, Chin C, Sotomi Y, Jonker H, Dijkstra J, Revalor E, Gijsen F, Onuma Y, Ooi A, Barlis P, Serruys PW. Endothelial shear stress 5 years after implantation of a coronary bioresorbable scaffold. *Eur Heart J*. 2018;39:1602–9.
20. Koskinas KC, Chatzizisis YS, Antoniadis AP, Giannoglou GD. Role of endothelial shear stress in stent restenosis and thrombosis: pathophysiologic mechanisms and implications for clinical translation. *J Am Coll Cardiol*. 2012;59:1337–49.
21. Waksman R, Zumstein P, Pritsch M, Wittchow E, Haude M, Lapointe-Corriveau C, Leclerc G, Joner M. Second-generation magnesium scaffold Magmaris: device design and preclinical evaluation in a porcine coronary artery model. *EuroIntervention J Eur Collab Work Group Interv Cardiol Eur Soc Cardiol*. 2017;13:440–9.
22. Neumann F-J, Sousa-Uva M, Ahlsson A, Alfonso F, Banning AP, Benedetto U, Byrne RA, Collet J-P, Falk V, Head SJ, Jüni P, Kastrati A, Koller A, Kristensen SD, Niebauer J, Richter DJ, Seferovic PM, Sibbing D, Stefanini GG, Windecker S, Yadav R, Zembala MO, ESC Scientific Document Group. 2018 ESC/EACTS Guidelines on myocardial revascularization. *Eur Heart J*. 2019;40:87–165.
23. Montone RA, Niccoli G, De Marco F, Minelli S, D'Ascenzo F, Testa L, Bedogni F, Crea F. Temporal Trends in Adverse Events After Everolimus-Eluting Bioresorbable Vascular Scaffold

Versus Everolimus-Eluting Metallic Stent Implantation: A Meta-Analysis of Randomized Controlled Trials. *Circulation*. 2017;135:2145–54.

24. Sorrentino S, Giustino G, Mehran R, Kini AS, Sharma SK, Faggioni M, Farhan S, Vogel B, Indolfi C, Dangas GD. Everolimus-Eluting Bioresorbable Scaffolds Versus Everolimus-Eluting Metallic Stents. *J Am Coll Cardiol*. 2017;69:3055–66.
25. Mejía-Rentería H, Lee JM, Lauri F, van der Hoeven NW, de Waard GA, Macaya F, Pérez-Vizcayno MJ, Gonzalo N, Jiménez-Quevedo P, Nombela-Franco L, Salinas P, Núñez-Gil I, Del Trigo M, Goto S, Lee HJ, Liontou C, Fernández-Ortiz A, Macaya C, van Royen N, Koo B-K, Escaned J. Influence of Microcirculatory Dysfunction on Angiography-Based Functional Assessment of Coronary Stenoses. *JACC Cardiovasc Interv*. 2018;11:741–53.
26. Quadri G, Tomassini F, Cerrato E, Varbella F. First reported case of magnesium-made bioresorbable scaffold to treat spontaneous left anterior descending coronary artery dissection. *Catheter Cardiovasc Interv Off J Soc Card Angiogr Interv*. 2017;90:768–72.
27. Quadri G, Cerrato E, Rolfo C, Varbella F. Spontaneous coronary artery dissection treated with magnesium-made bioresorbable scaffold: 1-Year angiographic and optical coherence tomography follow-up. *Catheter Cardiovasc Interv*. 2019;93:E130–3.
28. Ielasi A, Cerrato E, Geraci S, Campo G, Garro N, Leoncini M, Sganzerla P, Granata F, Ruggiero R, Varbella F, Caramanno G, Grigis G, Tespili M. Sirolimus-Eluting Magnesium Resorbable Scaffold Implantation in Patients with Acute Myocardial Infarction. *Cardiology*. 2019;142:93–6.

Table 1. Patient characteristics. Values are means ± Standard Deviations or n (%). DMT2: Diabetes Mellitus Type 2; CAD: Coronary Artery Disease; CABG: coronary artery bypass graft; PCI: percutaneous coronary intervention; MI: Myocardial Infarction; LVEF: Left Ventricular Ejection Fraction; CKD: Chronic Kidney Disease; ACS: Acute Coronary Syndrome; UA: Unstable Angina; NSTEMI: Non ST-Elevation Myocardial Infarction; STEMI: ST-Elevated Myocardial Infarction.

	N= 44
Male sex	38 (86.4)
Age	54.8 ± 7.5
DMT2	10 (22.7)
Insulin dependent DMT2	3 (6.8)
Hypertension	26 (59.1)
Dyslipidemia	20 (45.4)
Current smokers	22 (50)
Past smokers	8 (18.2)
Family history of CAD	14 (31.8)
Prior MI	17 (38.6)
Prior CABG	1 (2.3)
Prior PCI	17 (38.6)
Prior stroke	1 (2.3)
CKD	1 (2.3)
Ejection fraction	56.2 ± 7.1
Multivessel disease	24(54.5)
Clinical indication at hospital admission	
STEMI	7 (15.9)
NSTEMI	14 (31.8)
Unstable angina	2 (4.5)
ACS: PCI on culprit	23 (100)
Stable angina or silent ischemia	21 (47.3)
DAT at discharge	
Aspirin+clopidogrel	2(5)
Aspirin+prasugrel	19(43)
Aspirin+ticagrelor	23(52)

Table 2. Angiographic and procedural lesion characteristics. Values are means ± Standard Deviations or n (%). LAD: Left Anterior Descending; LCx: Left Circunflex; RCA: Right Coronary Artery; Type B2/C according to AHA Ellis classification; SB: Side Branch.

	N = 49
Target Vessel	
LAD	28 (57)
LCX	8 (16)
RCA	13 (27)
Segment	
Proximal	20 (41)
mid	17 (35)
distal	12 (24)
Type B2/C	47 (96)
Lesion length (visual)	32.2±17.2
Overlap (at least one)	21 (43)
Bifurcation (SB>2.0mm)	9 (19)
Predilatation	49 (100)
Pressure (atm)	19±3.3
Balloon diameter (mm)	3.2±0.3
Non-compliant balloon	48 (97.6)
Magmaris BrS	N=75
Pressure (atm)	12.7±1.0
Diameter (mm)	3.2±0.2
Length (mm)	34.9±17.8
Postdilatation	49 (100)
Pressure (atm)	21.9±4.7
Balloon diameter (mm)	3.4±0.4
Non-compliant balloon	48 (97.6)

Table 3. Quantitative Coronary Analysis (QCA), Quantitative flow ratio (QFR) and Optical Coherence Tomography (OCT) Findings. ISA: Incomplete Scaffold Apposition. MLA: minimal lumen area. MSA: minimal scaffold area. SE-RVA: scaffold expansion according to reference vessel area. Numbers are count (percentage), mean±Standard Deviation

QCA analysis	**Post-PCI**	**Follow-up**	**Δ 12 months vs post proc.**	**P-value**
Reference Vessel Diameter (mm)	2.97±0.34	2.94±0.32	-0.06 (-0.29-0.18)	0.025
Minimal Lumen Diameter (mm)	2.55±0.31	2.33±0.29	-0.02 (-0.45-0.05)	<0.01
Stenosis Diameter (mm)	14.0±5.9	20.7±8.9	5.1 (0.3-12.1)	<0.01
Acute gain (mm)	1.63±0.61	-	-	-
Late Lumen Loss (mm)	-	0.22±0.33	-	-
OCT analysis (n=42 lesions; 59 scaffolds)				
	Post PCI			
n°frame with malapposed struts	20			
ISA (mm^2)	0.03±0.23			
ISA length (mm)	0.12±0.09			
Overlap length (mm)	1.43±4.36			
Edge dissection (overall cases)	5			
Prox edge dissection max length (mm)	0.20±0.43			
Prox edge dissection max angle	15			
Distal edge dissection max length (mm)	1.2±0.4			
Distal edge dissection max angle	10			
Scaffold Fractures	0			
	Post PCI	**1 year Follow-up**	**Δ 12 months vs post proc.**	**p-value**
Mean Lumen Area (mm^2)	8.12±1.89	7.54±3.04	-0.88 (-1.93-0.38)	<0.01
MLA (mm^2)	6.31±1.70	4.60±1.55	-1.70 (-2.80- -0.89)	<0.01
MSA (mm^2)	6.23±1.69	-	-	-

Mean Scaffold area (mm^2)	8.08±1.83	-	-	-
Lumen max diam (mm)	3.47±0.42	3.37±0.71	-	<0.01
Lumen min diam (mm)	2.91±0.37	2.69±0.54	-	<0.01
Lumen mean diam (mm)	3.18±0.36	3.02±0.59	-	<0.01
Scaffold max diam (mm)	3.46±0.40	-	-	-
Scaffold min diam (mm)	2.91±0.37	-	-	-
Scaffold mean diam (mm)	3.18±0.36	-	-	-
SE-RVA (%)	79.3±12.2			
Eccentricity index	0.63±0.07			
Symmetry index	0.37±0.07			
OCT Resorption process analysis (n=42)		**1 year Follow-up;** n(%)		
Visible struts		0		
“golden tube” pattern		568 (42.4)		
“Humps” visible (at least one)		769 (57.6)		
1-4 “humps”		668 (86.9)		
≥5 “humps”		101 (13.1)		
Overall number of “humps”		1905		
QFR analysis (n=47)				
	Post PCI	**1 year Follow-up**		p-value
Contrast QFR	0.97±0.06	0.95±0.05		0.06
QFR > 0.80	46 (98)	46 (98)		1
QFR > 0.89	44 (93.6)	42 (89.4)		0.7

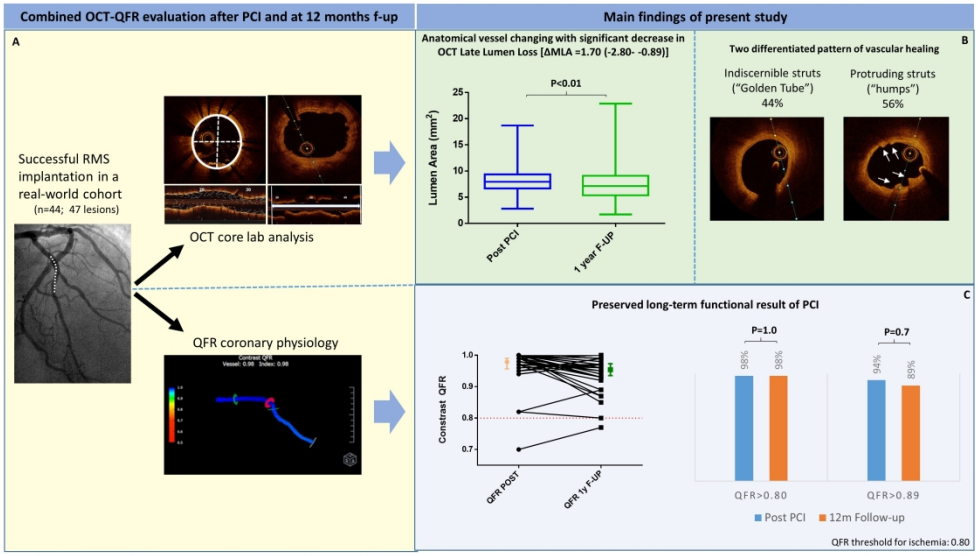

Figure 1, central illustration. Panel A: study flow-chart. Panel B: Optical Coherence Tomography (OCT) imaging findings post PCI and at 1-year follow-up. Panel C: Quantitative Flow Ratio (QFR) findings post PCI and at 1-year follow-up. * chi-square p value is reported using 0.80 as QFR threshold for ischemia.

338x190mm (300 x 300 DPI)

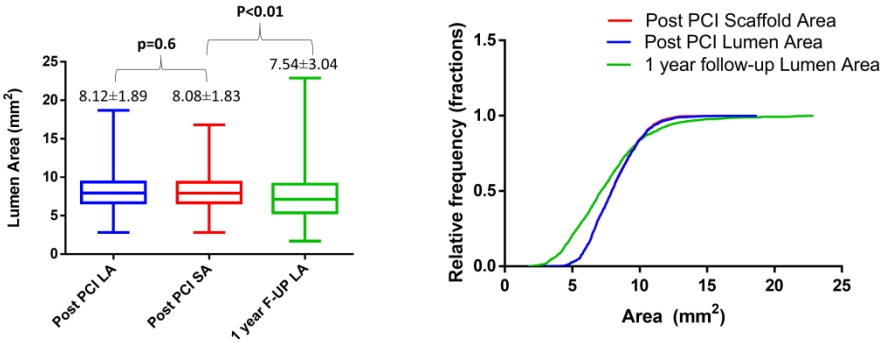

Figure 2: Imaging OCT findings. Left panel: boxplots for lumen / scaffold Area after PCI and at 1-year follow-up. Right panel: relative frequency distribution for lumen / scaffold area after PCI and at 1-year follow-up.

338x190mm (300 x 300 DPI)

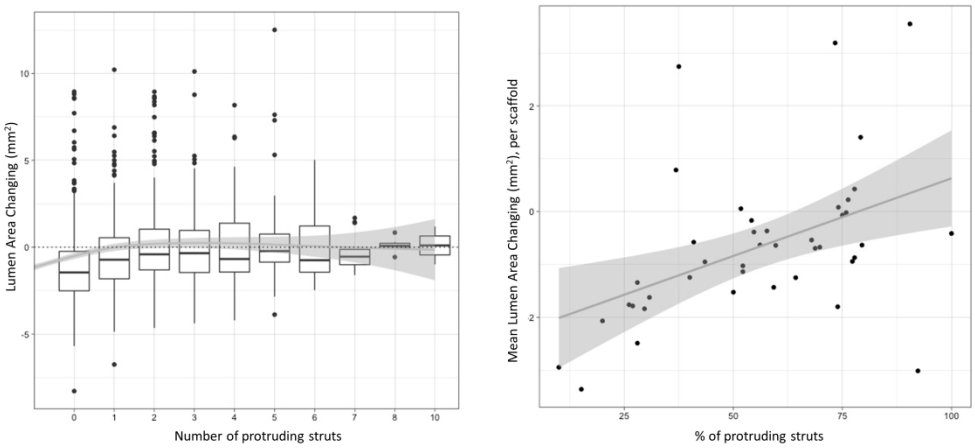

Figure 3. Left panel: distribution of the Lumen Area changing in mm2 (Lumen Area at follow-up - Lumen Area post PCI) for each number of protruding residual struts observed in each OCT frame. Boxes indicate 25% and 75% percentiles and the inner line marks the median. A dotted black line indicates a null gain and the grey line with shadow depicts the smoothed conditional means of Lumen Area changing given the number of protruding struts and the corresponding confidence interval. Right panel: mean Lumen Area (mm2) changing versus percentage of protruding residual struts per scaffold. The grey line corresponds to the least squares regression line with confidence interval.

338x190mm (300 x 300 DPI)

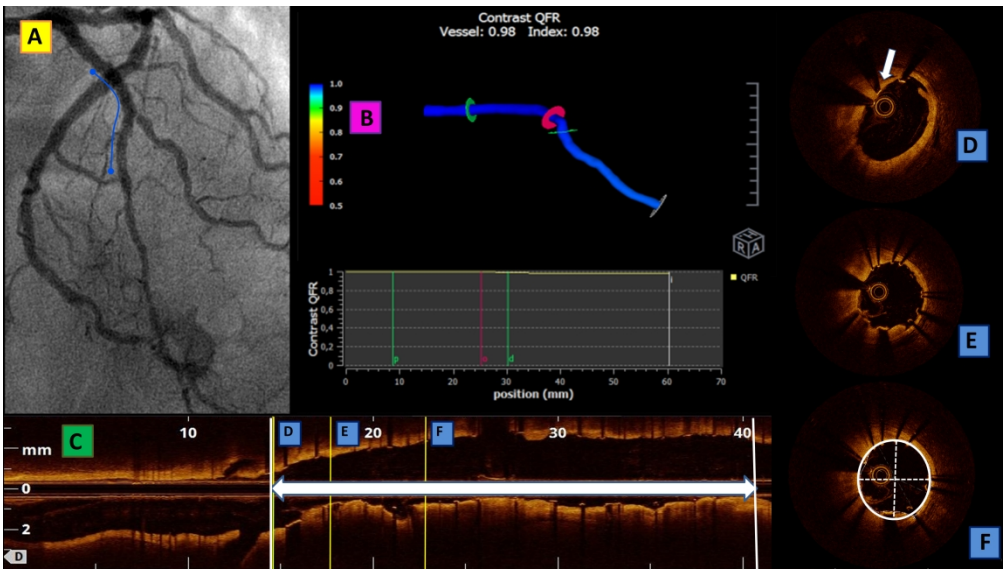

Figure A (Suppl material). Optical Coherence Tomography (OCT) and Quantitative Flow Ratio (QFR) post-PCI analysis. Picture A represents the angiographic result after Resorbable Magnesium Scaffold (RMS). The blue line shows the area of the vessel previously affected by stenosis where the scaffold was implanted. B: Post-PCI contrast QFR. C: Post-PCI OCT, longitudinal view. Picture C represents the longitudinal view of the area of the vessel where the scaffold was implanted, as seen using OCT. OCT images were analyzed at 1mm intervals, using tantallium BRS markers or struts as distal and proximal references of the scaffold. The vertical yellow lines show where the OCT trasversal images (D,E,F) are located along the vessel. D: Post-PCI OCT, trasversal view. Example of tantallium BRS marker, used as distal and proximal references of the scaffold to define the area of the vessel to analyze. E: Post-PCI OCT, trasversal view. OCT findings after the implantation of a RMS. F: Post-PCI OCT, trasversal view. Lumen area, maximum diameter and minimum diameter were registered each millimeter.

338x190mm (300 x 300 DPI)

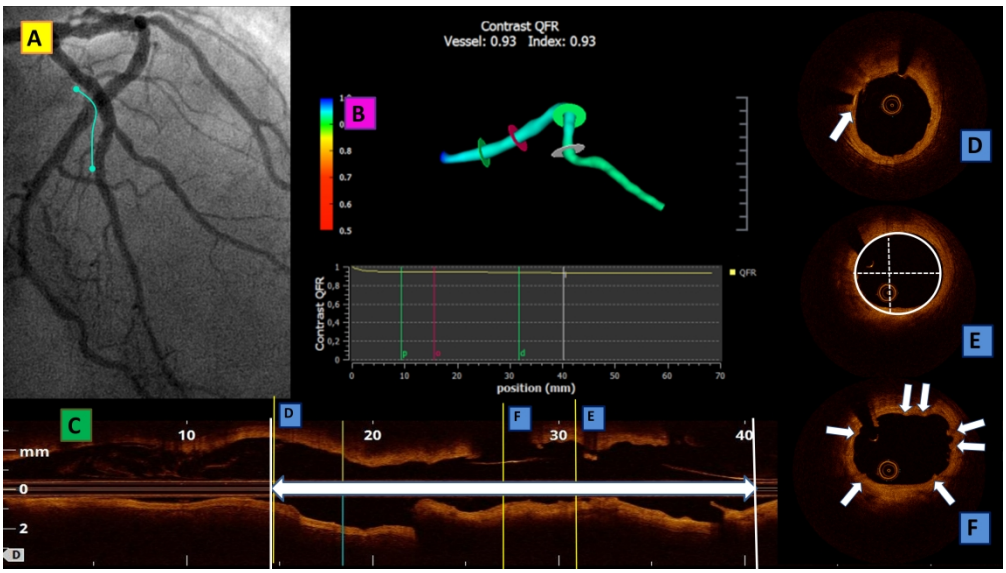

Figure B (Suppl material). Optical Coherence Tomography (OCT) and Quantitative Flow Ratio (QFR) one-year follow-up analysis

Picture A represents the 1-year result after Resorbable Magnesium Scaffold (RMS) implantation. The blue line shows the area where the scaffold was implanted. B: Follow-up contrast QFR. C: Follow-up OCT, longitudinal view. Picture C represents the longitudinal view of the area of the vessel where the scaffold was implanted, as seen using OCT. OCT images were analyzed at 1mm intervals, using tantallium BRS markers or struts as distal and proximal references of the scaffold. The vertical yellow lines show where the OCT trasversal images (D,E,F) are located along the vessel. D: Follow-up OCT, trasversal view. Example of tantallium BRS marker, used as distal and proximal references of the scaffold to define the area of the vessel to analyze. E: Follow-up OCT, trasversal view. Lumen area, maximum diameter and minimum diameter were registered each millimeter. F: Follow-up OCT, trasversal view. Presence of residual or protruding struts or in the vessel lumen was registered.

338x190mm (300 x 300 DPI)

Supplementary material

Supplement to: Anatomical and functional healing after Resorbable Magnesium Scaffold implantation in human coronary vessels: a combined optical coherence tomography (OCT) and Quantitative Flow Ratio (QFR) analysis.

Methods

Angiographic, Optical Coherence Tomography (QCT) and Quantitative Flow Ratio (QFR) methodology are summarized in supplemental figure A and B at the end of this appendix

Assessments and definitions

Quantitative angiographic analysis

Coronary angiograms were acquired following intracoronary injection of nitrates.

Offline QCA was performed with QAngio XA 3D/QFR solution (Medis medical imaging system bd., Leiden, The Newtherlands). Lesions were categorized according to ACC/AHA task force criteria for coronary lesion classification.

The following QCA parameters were obtained offline in the pre-procedural angiogram: Minimal Lumen Diameter (MLD), mean lumen diameter, percentage Diameter Stenosis (%DS) and Reference Vessel Diameter (RVD). RVD was defined as the maximum diameter (Dmax) between the 5 mm proximal and distal to the target lesion. Acute recoil was defined as the MLD achieved after complete expansion of the last balloon used for postdilatation (MLD1), minus the MLD at the end of the procedure (MLD2). The percentage of acute recoil was calculated with the following formula: ((MLD1-MLD2)/MLD1)*100. Late lumen loss (LLL) was calculated as the difference between the post-procedural and follow-up MLD, and angiographic binary restenosis defined as ≥ 50% in-device percent diameter stenosis (((RVD-MLD)/RVD)*100).

OCT imaging analysis

The analysis of contiguous cross-sections was performed at 1 mm longitudinal intervals within the entire scaffolded segment and at 5 mm intervals proximal and distal to the scaffold in order to measure the proximal and distal reference vessel area (RVA) and to identify dissections. RVA was calculated as the mean of the two largest luminal areas in the 5 mm proximal and distal to the BRS edge For each cross-section analysed, the area, mean, maximal and minimal diameter of the scaffold and of the lumen were automatically contoured and measured by the analysis system, with manual correction as appropriate. Baseline and follow-up pullbacks were matched per patient to obtain absolute and relative differences between measurements when available,

Lumen area (LA) was defined as the effective flow area, and the scaffold area (SA) was delineated by a curvilinear interpolation connecting the midpoints of the endoluminal leading edge. The reference vessel area (RVA) was calculated as the average of the maximum lumen area 5 mm proximal and distal to the scaffold edges. Minimal Lumen Area (MLA) and Minimal Scaffold Area (MSA) were defined as the smallest lumen and scaffold areas within the scaffolded segment.. Scaffold expansion (SE) according to RVA (SE-RVA) was defined as (MSA/RVA)*100 and SE according to MEA (SE-MEA) was defined as (MSA/MEA)*100. Scaffold eccentricity index was computed as the average of all eccentricity indices (ratio between the minimum and maximum diameter per frame) and scaffold symmetry index was defined as (maximum scaffold diameter-minimum scaffold diameter)/maximum scaffold diameter. Incomplete strut apposition (ISA) was identified when the distance between the endoluminal surface of the struts with respect to the intima layer was greater than the strut thickness. Scaffold edge dissection was defined as a disruption of the vessel luminal surface at the scaffold edge with visible flap. Malapposed

struts are defined as a distance between the strut marker and lumen contour greater than the strut thickness plus the axial resolution of OCT. Scaffold fracture was suspected in the presence of isolated struts lying grossly unapposed in the lumen or in the presence of one strut on top of the other.

Per-scaffold analysis: Mean Lumen difference was defined as a mean of all lumen areas at follow-up minus all lumen areas after PCI. Scaffold Volume is defined as the sum of all lumen areas in each analysed scaffold. Mean volume gain was defined as the mean of scaffold Volume at follow-up minus the mean of scaffold Volume after PCI

Supp. table A. Baseline features of patients included and excluded from the analysis. Values are means ± Standard Deviations or n (%). DMT2: Diabetes Mellitus Type 2; CAD: Coronary Artery Disease; CABG: coronary artery bypass graft; PCI: percutaneous coronary intervention; MI: Myocardial Infarction; LVEF: Left Ventricular Ejection Fraction; CKD: Chronic Kidney Disease; ACS: Acute Coronary Syndrome; UA: Unstable Angina; NSTEMI: Non ST-Elevation Myocardial Infarction; STEMI: ST-Elevated Myocardial Infarction.

	Included in the analysis N= 44	**Excluded from the analysis N=34**	**P value**
Male sex	38 (86.4)	26 (76.5)	0.214
Age	54.8 ± 7.5	57.2 ± 9.2	0.204
DMT2	10 (22.7)	4 (11.8)	0.147
Insulin dependent DMT2	3 (6.8)	1 (2.9)	0.387
Hypertension	26 (59.1)	19 (55.9)	0.563
Dyslipidemia	20 (45.4)	20 (58.8)	0.331
Current smokers	22 (50.0)	13 (38.2)	0.121
Past smokers	8 (18.2)	8 (23.5)	0.227
Family history of CAD	14 (31.8)	8 (23.5)	0.532
Prior MI	17 (38.6)	16 (47.1)	0.694
Prior CABG	1 (2.3)	0	0.353
Prior PCI	17 (38.6)	18 (52.9)	0.370

Prior stroke	1 (2.3)	1 (2.9)	0.907
CKD	1 (2.3)	0	0.802
Ejection fraction	56.2 ± 7.1	56.4 ± 7.8	0.563
Multivessel disease	24(54.5)	20 (58.8)	0.918
Clinical indication at hospital admission			0.102
STEMI	7 (15.9)	2 (5.9)	
NSTEMI	14 (31.8)	6 (17.6)	
Unstable angina	2 (4.5)	3 (8.8)	
Stable angina or silent ischemia	21 (47.3)	23 (67.6)	
ACS: PCI on culprit	23 (100)	11 (100)	1.000
DAT at discharge			0.082
Aspirin+clopidogrel	2(5)	11 (32)	
Aspirin+prasugrel	19(43)	1 (3)	
Aspirin+ticagrelor	23(52)	13 (38)	

Supp. table B. Angiographic and procedural lesion characteristics of patients included and excluded from the analysis. Values are means ± Standard Deviations or n (%). LAD: Left Anterior Descending; LCx: Left Circunflex; RCA: Right Coronary Artery; Type B2/C according to AHA Ellis classification; SB: Side Branch.

	N = 49	**N=44**	**P value**
Target Vessel			0.191
LAD	28 (57)	24 (54)	
LCX	8 (16)	8 (18)	
RCA	13 (27)	12 (25)	
Segment			0.105
Proximal	20 (41)	15 (34)	
mid	17 (35)	22 (51)	
distal	12 (24)	7 (16)	
Type B2/C	47 (96)	39 (89)	0.802
Lesion length (visual)	32.2±17.2	33.0±16.1	0.599
Overlap (at least one)	21 (43)	15 (43)	0.982
Bifurcation (SB>2.0mm)	9 (19)	8 (23)	0.532
Predilatation	49 (100)	43 (97.7)	0.315
Pressure (atm)	19±3.3	19±3.4	0.171
Balloon diameter (mm)	3.2±0.3	3.1±0.2	0.458
Non-compliant balloon	48 (97.6)	42 (95.5)	0.678

Magmaris BrS	N=75	N=75	
Pressure (atm)	12.7±1.0	12.9±1.1	0.231
Diameter (mm)	3.2±0.2	3.3±0.3	0.224
Length (mm)	34.9±17.8	35.8±15.8	0.640
Postdilatation	49 (100)	44 (100)	1.000
Pressure (atm)	21.9±4.7	20.9±4.4	0.782
Balloon diameter (mm)	3.4±0.4	3.4±0.5	0.680
Non-compliant balloon	48 (97.6)	44 (100)	0.523

Other contributors list:

Interventional Cardiology Unit, San Luigi Gonzaga University Hospital, Orbassano and Rivoli Infermi Hospital, Rivoli (Turin), Italy

Luca Lo Savio, Alfonso Franze', Fabio Mariani, Francesco Tomassini

Division of Cardiology, "Città della Salute e della Scienza di Torino" Hospital, Department of Medical Sciences, University of Turin, Italy

Laura Montagna